Supplementary Data

Factors determining DNA double strand break repair pathway choice in G2 phase.

Atsushi Shibata[1], Sandro Conrad[2], Julie Birraux[1], Verena Geuting[2], Olivia Barton[2], Amani Ismail[1], Andreas Kakarougkas[1], Katheryn Meek[3] Gisela Taucher-Scholz[4], Markus Löbrich[2*] and Penny A. Jeggo[1*]

Figure S1. Analysis of IR induced foci (IRIF) in G1 and G2 cells.
A and B) Aphidicolin (APH) was added immediately after 2 Gy X-rays. APH treatment blocks the replicative polymerases and hence progression from S to G2 phase. APH induced replication stress induces an obvious pan-nuclear γH2AX/RPA signal in S phase (Beucher et al, 2009). Cells are stained with γH2AX or RPA and CENP-F (a G2 marker). G1 cells show very low CENP-F signal and clear IRIF. Early S cells show very low CENP-F signal but strong pan-nuclear γH2AX/RPA signal. Late S phase cells have a mild CENP-F signal + pan-nuclear γH2AX/RPA signal. G2 cells have a greater CENP-F signal and clear γH2AX/RPA IRIF. M phase cells are distinguished from other cell cycle phases by morphology and cytoplasmic CENP-F signal. APH does not affect DSB repair including γH2AX, RPA, Rad51 foci formation or SCE formation in cells derived from G2 phase cells and blocks cell cycle progression from S to G2 even in checkpoint defective cells. Full controls for the use of APH have been included in (Beucher et al, 2009; Shibata et al, 2010).

Figure S2. IR induced RPA/Rad51 foci co-localise with DSBs in G2 phase.
A) Cells were irradiated with 2 Gy X-rays and APH added immediately. Visible RPA foci were not detected until ~2 hr after X-rays. However IR induced RPA foci at >2 hr strongly co-localize with the DSB marker, 53BP1.
B) IR induced γH2AX and 53BP1 co-localize in G2 cells.
C) IR induced Rad51 foci at >2 hr co-localize with γH2AX foci. The number of RPA foci at 2 h post X-rays is similar to the number of unrepaired DSBs in HR defective cells (e.g. BRCA2 cells) (which is also identical to the number of unrepaired DSBs in ATM defective cells). Additionally, NHEJ defective cells are impaired in the fast component of DSB repair in G2 phase. Thus we enumerate RPA/Rad51 foci at >2 hr after IR as a monitor of resection. We relate this to the number of DSBs induced as assessed by γH2AX numbers 15 min post treatment in Figure 1.

Figure S3. Substantial persistent RPA foci and a DSB repair defect in HR defective cells after carbon-ion irradiation.
A) Cells were irradiated with 2 Gy carbon ions, and stained with RPA and CENP-F. 50% of RPA foci were repaired at 24 hr post carbon irradiation in wild type cells (Figure 1D). In contrast, >90% of RPA foci remained up to 24 hr post carbon irradiation in BRCA2 deficient cells. Importantly, the number of RPA foci at 24 hr in BRCA2 deficient cells is not drastically changed compared to 2 hr, indicating that the number of RPA foci at 2 hr

represents the peak of RPA foci formation. This result also suggests that carbon ion induced DSBs that become associated with RPA are repaired by BRCA2 dependent HR.
B) >~90% of γH2AX foci persist in *Rad54*$^{-/-}$ MEFs up to 24 h post carbon-ion irradiation. The number of γH2AX foci was enumerated after 2 Gy carbon ions. These results indicate that DSB repair post carbon ions is repaired by BRCA2/Rad54 dependent HR. G2 cells were identified as speckled p-histoneH3 Ser10 staining in MEFs.
C) The kinetics of DSB repair was examined by enumerating γH2AX foci in HSF1 primary cells in G1 (left) or G2 (right) cells. % of repair kinetics is shown in Figure 1A and B. Cells were exposed to 2 Gy carbon ions, 2 Gy X-rays and 20 (for G1) or 5 μM (for G2) Etp for 15 min and stained with γH2AX and CENPF. *The number of γH2AX foci post carbon ions was examined at the indicated time points except for 6 hr.
D) RPA or Rad51 foci numbers in G2 phase were enumerated following exposure to 2 Gy carbon ions, 2 Gy X-rays and 5 μM Etp in HSF1 primary cells. % of RPA or Rad51/γH2AX foci at 15 min is shown in Figure 1C. The doses chosen generate similar numbers of γH2AX foci at 2 h after treatment, since RPA/Rad51 foci numbers reach the maximal levels at 2 hr post treatment as discussed in Supplementary Figure S2. The induction of DSB formation after carbon ion irradiation might be underestimated if they arise in close proximity. Nevertheless, importantly, given that we observe fewer not more γH2AX foci, it is unlikely that this can explain the magnitude of the increase in RPA/Rad51 foci that we observe. *The number of RPA post carbon ions was examined at the indicated time points except for 6 hr.

Figure S4. Etp can induce HC-DSBs, but they are 2-3 fold lower than X-ray-induced HC-DSBs.
A) Not all persistent γH2AX foci co-associate with pKAP-1 foci. Cells lacking XLF, a core NHEJ protein, were exploited to examine a situation where EC and HC-DSBs might persist. At 8 h post 30 μM Etp. for 30 min, the % of pKAP-1 positive γH2AX foci is approximately 20% in XLF cells, which corresponds to the percentage of HC-DNA. Since Etp induces a lower percentage of HC-DSBs, 1BR (WT) hTERT cells were treated with 150 μM Etp for 30 min, which results in ~8 γH2AX foci remaining at 8 hr similar to the number remaining in XLF cells treated as described above. In these 1BR hTERT cells nearly all (84 %) of γH2AX foci co-localise with pKAP-1 foci. Thus, pKAP-1 does not form at all persisting γH2AX foci. Rather, those persisting in control cells represent the slowly repaired HC-DSBs.
B) Etp can induce DSBs at HC regions in NIH3T3 cells. To induce a similar number of DSBs (~30 γH2AX foci), cells were treated with 20 μM Etp 30 min or irradiated with 1 Gy X-rays. After fixation, cells were stained for γH2AX (green) and DAPI (blue). γH2AX (red) in right panel represents regions of γH2AX and dense-DAPI chromocentre overlap as determined by softWoRx® Suite software. Etp induced DSBs can localise to densely staining DAPI regions but the percentage is less than for X-ray induced DSBs.

Figure S5. Analysis of RPA foci in Ku80+BRCA2 siRNA cells. DNA-PK expression in CHO V3 cell lines.

A) Ku80 siRNA significantly increases RPA foci numbers post IR. Quantification is shown in Figure 3A. Knockdown efficiency was assessed by immunoblot as shown in right panel. β-tubulin was used as a loading control.
B) DNA-PKcs expression levels in CHO V3 cell lines. DNA-PKcs null hamster V3 cells express human DNA-PKcs with or without mutations in the ABCDE phosphorylation sites. Ku80 and β-tubulin were used as a loading control. The level of DNA-PKcs expression between V3+ WT and particularly between the V3+ABCDE S>D mutant and V3-ABCDE S>A mutant is similar but the magnitude of resection at 1 h post treatment is very different. The signal intensity of DNA-PKcs was quantified with ImageJ. Normalized signal intensities with Talin (cytoskeletal protein) are shown on the bottom of the blots.

Figure S6. CtIP siRNA leads to reduced IR induced Rad51 foci formation in G2 but does not affect activation of ATM signalling.
A) Cells were irradiated with 3 Gy IR, and stained with Rad51 and CENP-F. Cells containing >5 Rad51 foci were scored as positive. Consistent with ablated RPA foci formation following CtIP siRNA treated cells, CtIP siRNA also significantly reduced Rad51 foci formation (right panel).
B) CtIP siRNA reduced Chk1 S317 phosphorylation, but did not affect ATM dependent pKAP-1 S824 and pChk2 T68. Further, IR induced pATM S1981 foci form normally in CtIP knockdown G1 and G2 cells.

Figure S7. A model for the regulation of DSB repair pathway usage at two-ended DSBs in G2.
We propose that both DNA damage complexity and chromatin complexity can influence the speed of DSB repair and that DSBs, which are not efficiently rejoined by NHEJ, preferentially undergo DSB end-resection. 1) DSBs that arise in EC-DNA without high DNA complexity undergo efficient repair with faster kinetics by NHEJ regardless of cell cycle phase. 2) when a highly complex DSB arises in EC-DNA, it is repaired with slow kinetics in both G1 and G2. In G2, NHEJ stalls and the DSBs undergo resection and subsequent repair by HR. 3) HC is also a barrier slowing repair by NHEJ. In G1 phase, an HC-DSB is repaired slowly by NHEJ. In G2 phase, NHEJ stalls, allowing resection and subsequent repair by HR. Repair pathway usage at an HC-DSB can be switched from HR to NHEJ when CtIP dependent DSB end resection does not occur. Whereas CtIP-dependent resection commits to HR. ATM has direct and indirect roles in regulating DSB end resection by promoting KAP-1 dependent heterochromatin relaxation and by activating CtIP by phosphorylation.
The precise magnitude of DNA damage complexity required to stall or slow NHEJ is currently unclear but the association of base damage at DSBs does not appear to restrict NHEJ usage since most X or γ-ray induced DSBs fall into this class. Additionally, it is unclear whether there is an impact of lesion complexity on HC-DSBs – e.g. whether DSBs without any additional lesions can be repaired rapidly (and without undergoing resection) in G2 phase. Our findings do not eliminate the possibility that some Etp-induced DSBs arising in HC-DNA can be repaired with fast kinetics without undergoing resection.

Table. S1 Comparison of DSB repair kinetics between Etoposide and γ-ray induced damage

	Etoposide	γ-ray
Induction of γH2AX foci	~150	42.3
No. of pKAP-1 associated γH2AX foci at 8 hr	6.9	5.3
% of pKAP-1 associated DSBs at 8 h	~4.6%	12.6%
Half-life of faster repair kinetics	~2.2 h	1.5 h*
Half-life of slower repair kinetics	12.7 h	10.2 h*

*The data of γ-ray are from Noon et al., NCB, 2010.

References.

Beucher A, Birraux J, Tchouandong L, Barton O, Shibata A, Conrad S, Goodarzi AA, Krempler A, Jeggo PA, Lobrich M (2009) ATM and Artemis promote homologous recombination of radiation-induced DNA double-strand breaks in G2. *EMBO J* **28**(21)**:** 3413-3427

Shibata A, Barton O, Noon AT, Dahm K, Deckbar D, Goodarzi AA, Lobrich M, Jeggo PA (2010) Role of ATM and the damage response mediator proteins 53BP1 and MDC1 in the maintenance of G(2)/M checkpoint arrest. *Mol Cell Biol* **30**(13)**:** 3371-3383

Supplementary Figure S1

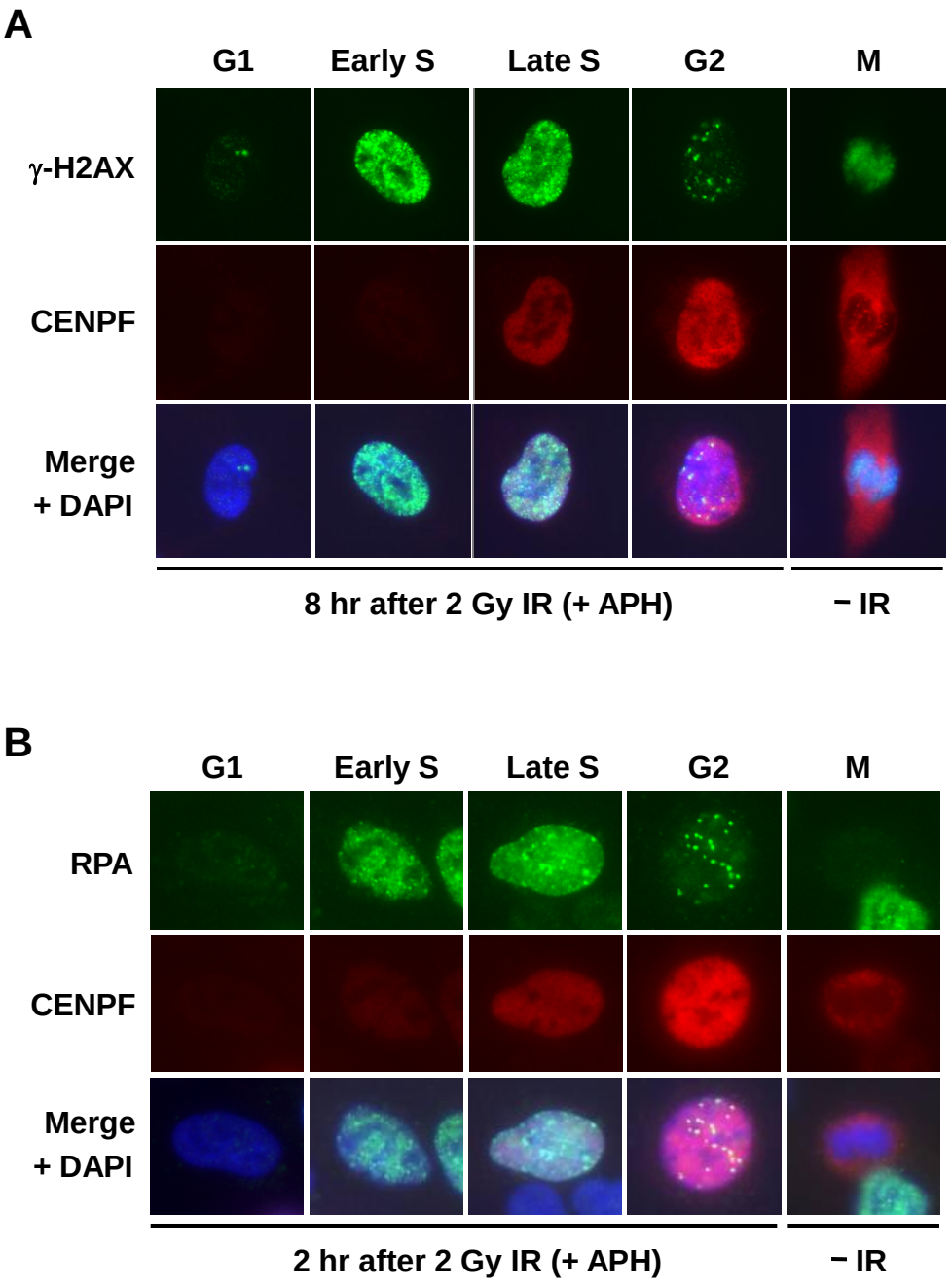

Supplementary Figure S2

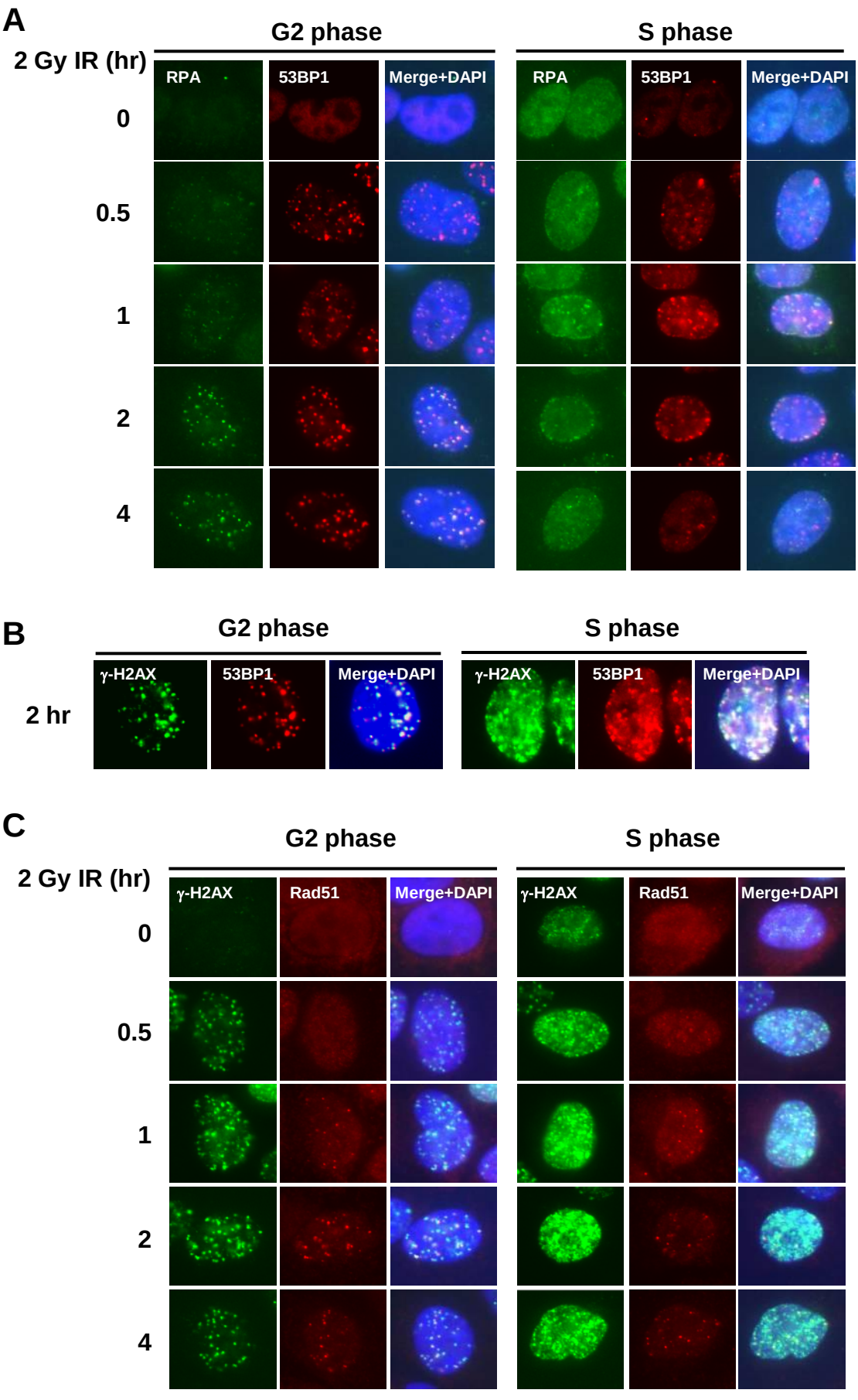

Supplementary Figure S3

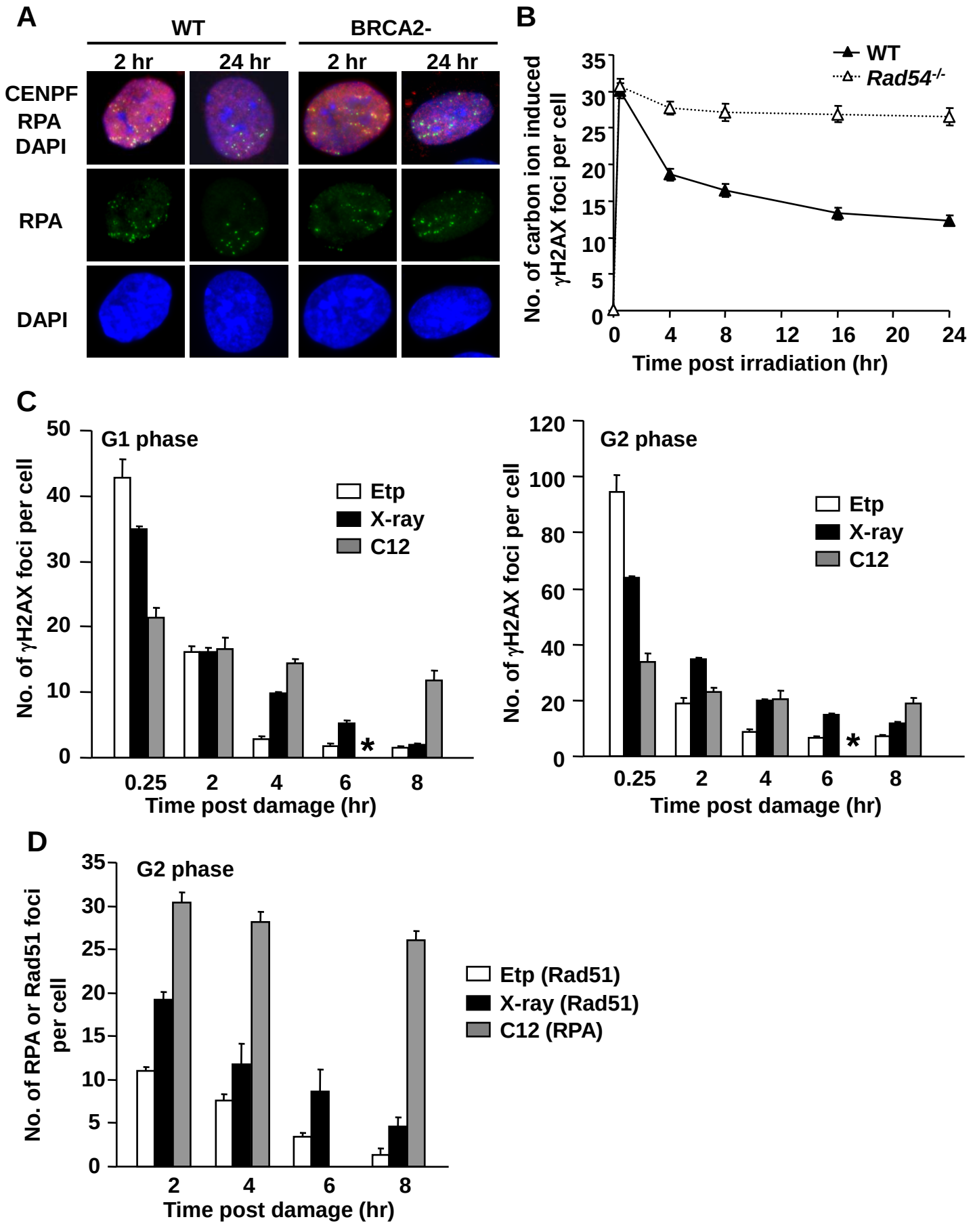

Supplementary Figure S4

A

pKAP-1 associated γH2AX / Analysed no. of γH2AX foci

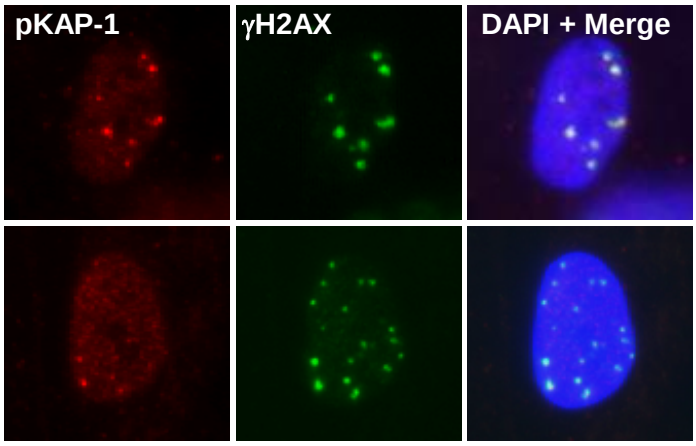

1BR (WT) hTERT
8 hr
post 150 μM Etp

151/181
(83.4%)

XLF hTERT
8 hr
post 30 μM Etp

38/173
(21.9%)

B

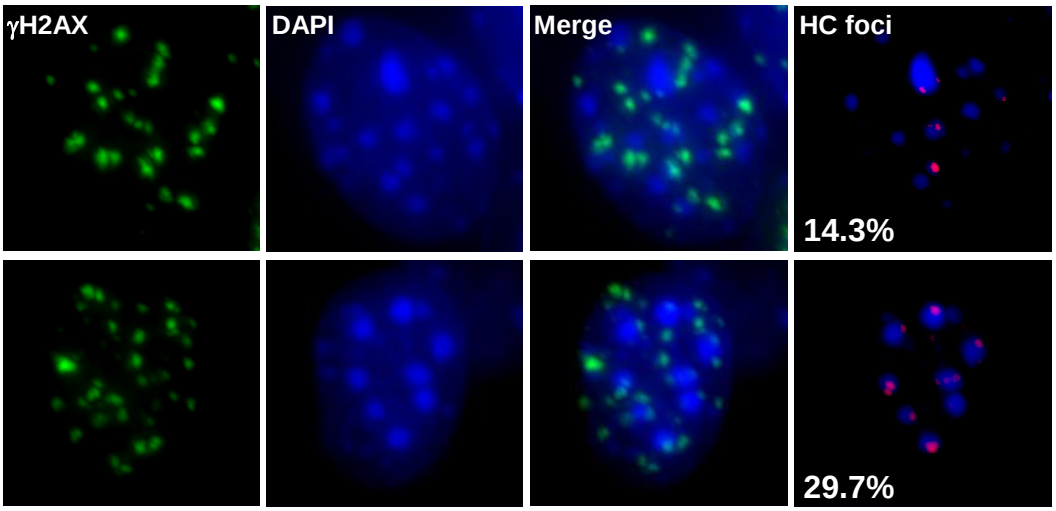

20 μM Etp

1 Gy X-ray

*% of HC-γH2AX foci

Supplementary Figure S5

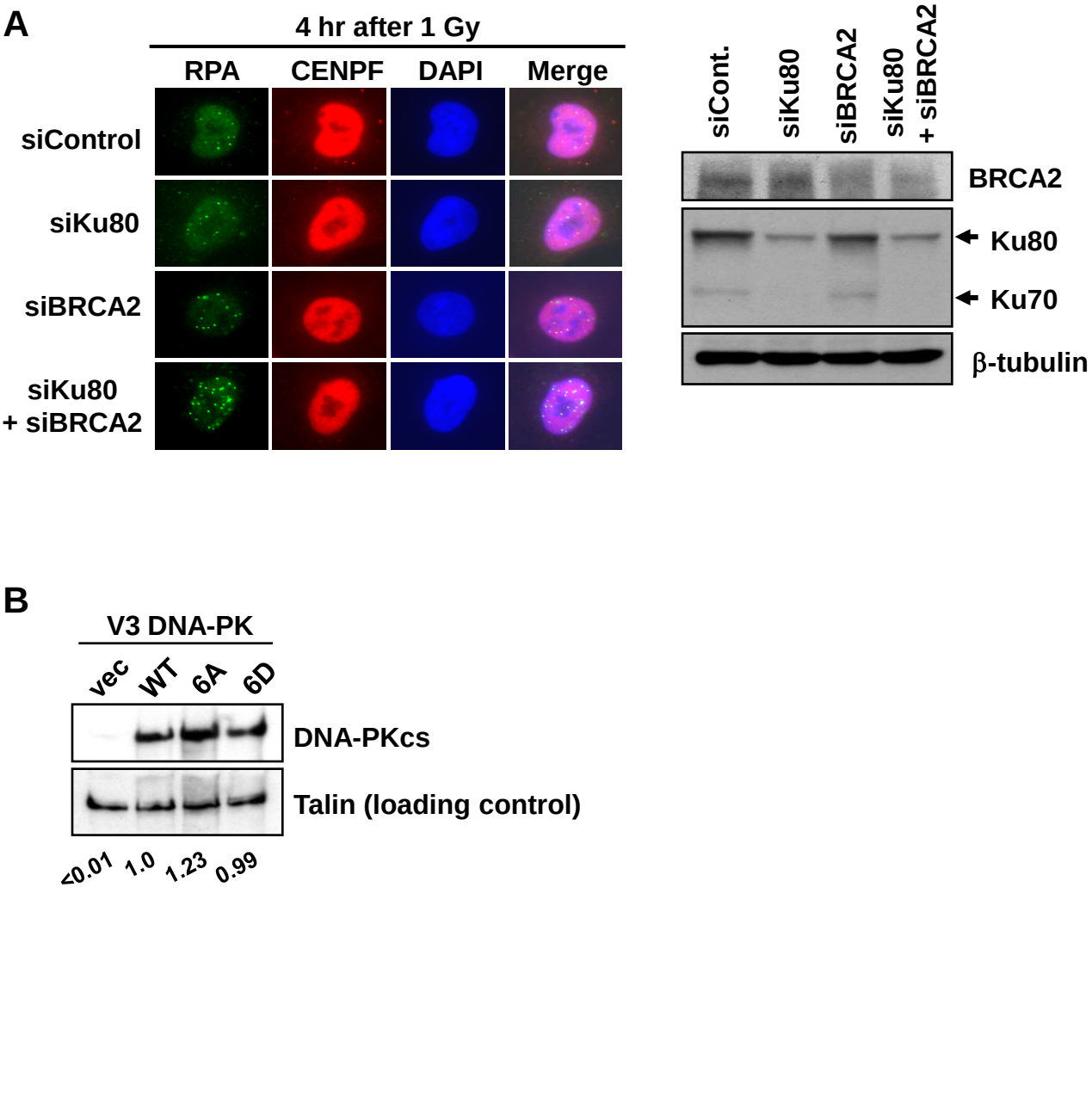

Supplementary Figure S6

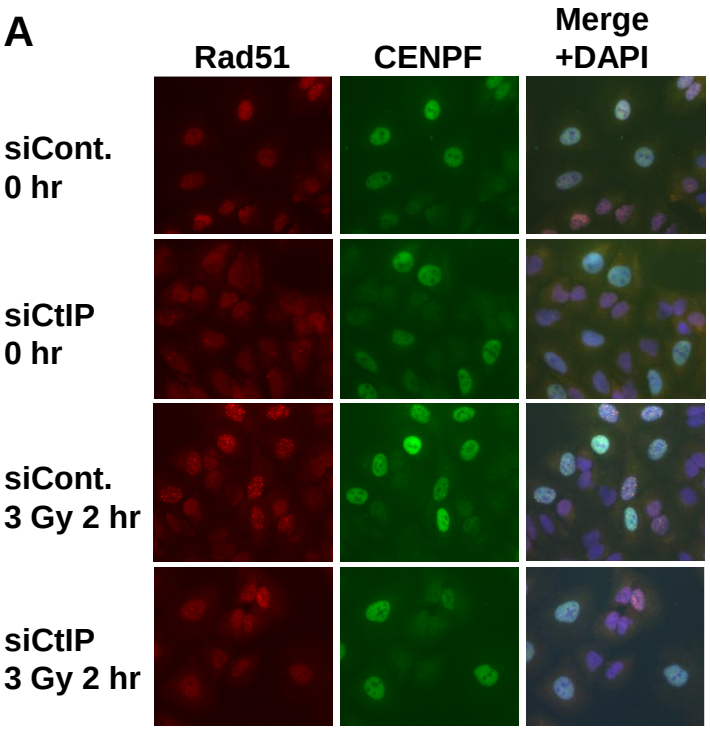

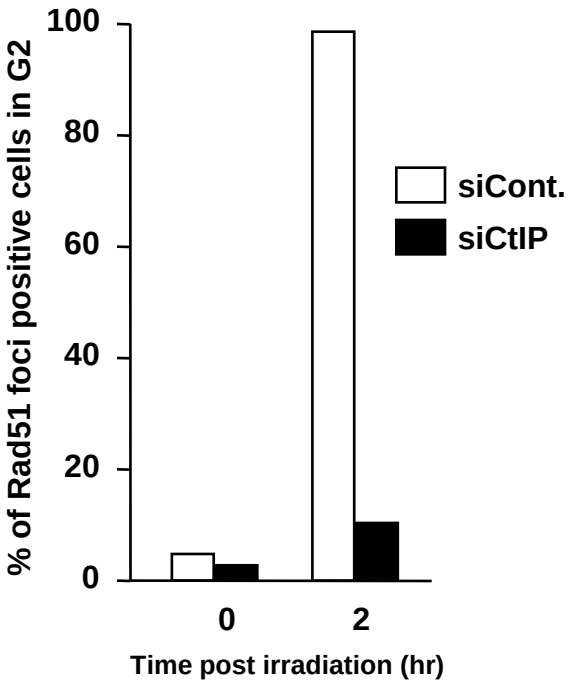

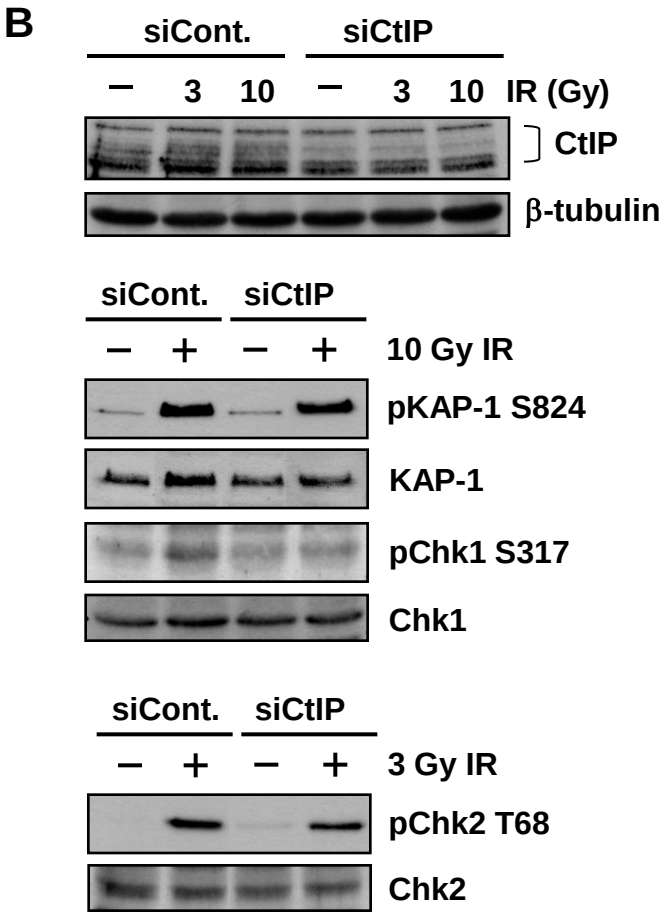

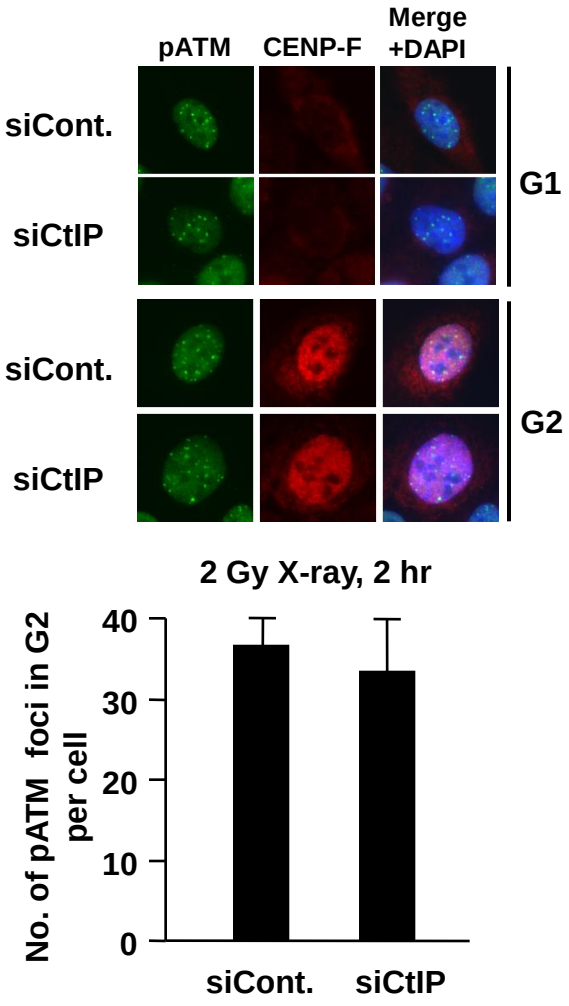

Supplementary Figure S7